

COMBINED OPTIMIZATION OF A LINAC-BASED FEL LIGHT SOURCE USING A MULTIOBJECTIVE GENETIC ALGORITHM*

Christos F. Papadopoulos[†], Daniele Filippetto, Gregory Penn,
Ji Qiang, Fernando Sannibale, Marco Venturini
LBNL, 1 Cyclotron Road, Berkeley, CA 94720, USA

Abstract

We report on the development status and preliminary results of a combined optimization scheme for a linac-based, high repetition rate, soft X-ray FEL. The underlying model includes the injector and linac parts of the machine, and the scheme will integrate the design process of these components toward the optimization of the FEL performance. For this, a parallel, multi-objective genetic algorithm is used. We also discuss the beam dynamics considerations that lead to the choices of objectives, or figure-of-merit beam parameters, and describe numerical solutions compatible with the requirements of a high repetition rate user facility.

INTRODUCTION

The development of 4th generation light sources based on the Free Electron Laser (FEL) concept requires high electron beam quality, as quantified by the transverse emittance and energy spread of the electron beam. In particular, for the case of seeded and echo-enabled harmonic generation, the requirements for the energy spread become even stricter [1].

These requirements on the beam can be straightforwardly transformed to a multi-objective optimization problem, since there is an intrinsic trade-off between transverse and longitudinal beam quality, as a consequence of the conservation of 6-dimensional phase space density due to Liouville's theorem [2]. In addition to this, the complexity of the machine, as well as the different physical models relevant for different parts of the accelerator form a coupled, complex system with a multitude of “knobs” available. For this, a combined optimization approach, based on genetic algorithms [3], is relevant.

In particular, the concept of a Pareto front [4], is useful, as it provides a way to visualize the trade-offs in different objectives (these are the quantities that we are trying to minimize) among a population of solutions. In the ideal case, the Pareto front in 2 dimensions is a 1 dimensional curve, and all solutions along it are optimal, in the sense that decreasing one of the objectives will increase the other. This concept can be generalized in a straightforward way to higher dimensions.

The choice of one or more solutions out of the optimal population is consequently based not only on the values of

the objective quantities, but also on the overall properties of the solution. In our case, we use the final phase space plots of the beam at the exit of the injector or the linac, since they contain significant information about the beam structure. For the numerical estimation of this front of solutions, there exist a number of algorithms, and in our case we use the NSGA2 algorithm described in [4].

In this paper, the focus will be on combining the optimization efforts for the first two parts of the electron accelerator, namely the injector part, up to an energy of around 70 MeV, and the linac and compressor part, with beam energy increasing from 70 MeV to higher than 1.8 GeV. The ultimate goal will be to optimize the beam characteristics at the entrance of the FEL undulators.

HIGH REP. RATE PHOTOINJECTOR

Injector Layout

The design of the injector is based on the VHF (187 MHz) gun, an RF gun running in continuous wave (CW) mode, which is described in [5]. The electron gun is specifically developed to allow operation at a high rep. rate of around 1 MHz. A schematic of the design is shown in Fig. 1.

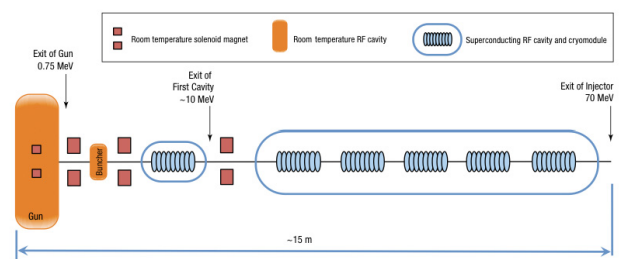


Figure 1: Conceptual design of the high rep. rate injector.

In addition to the electron gun, a beamline consisting of two solenoids, one single-cell cavity and 6 nine-cell cavities constitute the injector. The solenoids are used for emittance compensation and transverse confinement of the beam, and depending on the transverse confinement needs there may be two or three. The single-cell and first two of the nine-cell cavities are dephased with respect to the maximum acceleration phase, in order to imprint a time-energy correlation to the beam and achieve ballistic and velocity

* This work was supported by the Director of the Office of Science of the US Department of Energy under Contract no. DEAC02-05CH11231

[†] cpapadopoulos@lbl.gov

bunching, or compression, respectively. The energy at the exit of the injector hence depends on the particular optimized solution, and is typically around 70 MeV. As in the case of the downstream linac, the RF cavities upstream of the VHF gun operate at 1.3 GHz.

Injector Optimization

The main goal of the injector design is to transport the beam up to relativistic energies, where space charge effects become less important, since in general they scale as I/γ^3 , where I is the beam current and γ the relativistic factor. For the set of parameters discussed, this happens at energies larger than 70 MeV. The numerical code used to model the low energy part of the accelerator is ASTRA [6], a widely used and benchmarked tool for simulating space-charge dominated dynamics.

As is well known [2], at low energies the nonlinear space charge forces can increase the transverse emittance of the beam. At the same time, the requirement for high current at the FEL means that significant part of the compression needs to be done at low energies, hence increasing the beam current I . Thus, beam emittance and beam pulse length form a set of optimization objectives that, intuitively, work against each other, and are a good match for a multi-objective algorithm. In order to decouple the phase space quality from the beam energy, the normalized rms emittance is used as a figure of merit instead of the energy-dependent geometric emittance. At the end of the runs, the slice, i.e. time dependent, values of the emittance are considered, since they play an important role for the relatively long pulses required in the final FELs.

The knobs used include the strengths of the solenoids, the phases and gradients of the single cell and the first 2 of the accelerating cavities, as well as the bunch length and transverse size of the beam at the cathode, which can be controlled through laser shaping. Thus, the total number of knobs can be as high as 15.

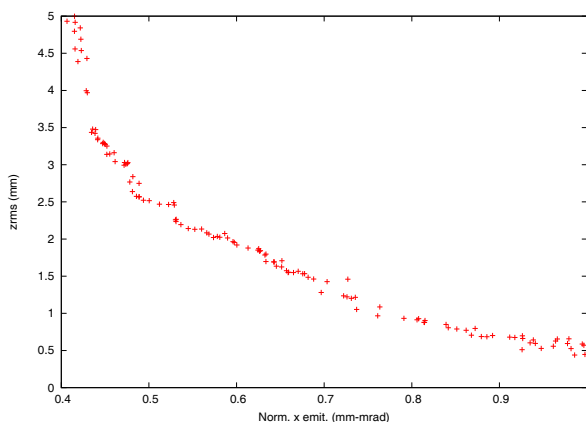


Figure 2: Pareto optimum front at the exit of the injector (70 MeV) for a 300 pC bunch.

From the Pareto front of optimal solutions in Fig. 2, we

pick one solution, shown in Fig. 3. The choice is driven by the current and minimal nonlinear correlations in the longitudinal phase space. The normalized slice emittance of the beam, with the exception of the head is less than 0.6 mm-mrad.

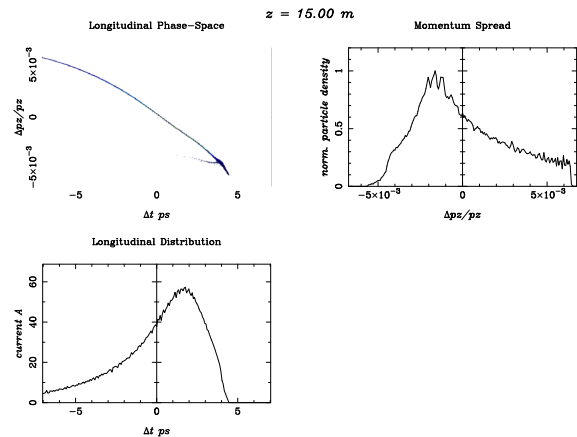


Figure 3: Longitudinal phase space and projections for a solution at the injector exit. The head of the beam is in the right.

SUPERCONDUCTING LINAC

Linac Layout

The linac section of the accelerator is defined as the part between the injector, at 70 MeV, and the FEL undulator lines, designed for energies equal or higher than 1.8 GeV. It comprises of 6 sections, namely the linac 1 (the first accelerating part, with superconducting TESLA-like cavities operating at 1.3 GHz), a third-harmonic RF cavity operating at 3.9 GHz, a single bunch compressor, linac 2, and finally the spreader, where fast kickers distribute the beam to different FEL lines. In addition to this, a laser heater is also accommodated, as it has been proven useful for the control of the microbunching instability. This is a close variant of the linac model discussed in [7]. The single bunch-compressor linac design considered here, which is known to present some benefits in terms of minimization of the microbunching instability, is one of the several options that we intend to thoroughly investigate in the future. The optimizer algorithm is fully capable of handling more bunch compressors, and to quickly and efficiently compare the relative merits of different designs.

Linac Optimization

The main operation of the linac part of the accelerator is to accelerate the beam to energies larger than 1.8 GeV, and compress it to short bunches, resulting in peak current larger than 500 A. During this process the transverse and longitudinal quality of the phase space must be conserved.

The numerical code used to model the beam dynamics in this case is Elegant, a thoroughly benchmarked code well

suites for the study of electron beams in the relevant energy scales [9]. The input distribution chosen is the realistic distribution generated from the injector optimization, as shown in Fig. 3. The number of particles for the linac run can be larger than the case of the injector, since the transverse space charge forces needed at lower energies are no longer as strong, and can thus be omitted at higher energies. For this, the injector solution is recalculated with higher accuracy, and shows agreement with the lower accuracy case for the beam core in the transverse and longitudinal projections.

The same multi-objective genetic algorithm is used to optimize the linac settings. In this case though, we use 3 objectives, namely the rms bunch length, the total momentum spread expressed in the dimensionless form $\delta = dp/p$, and the average slice momentum spread of the beam, again in terms of δ , at the exit of the spreader. A fourth objective, the transverse emittance will be added in future implementations of the algorithm. One additional constraint is that the beam energy at the spreader exit should not be less than 1.8 GeV.

The knobs available for the linac optimization are the phases and gradients of the cavities in linac 1 and 2, as well as the ones for the third harmonic cavity linearizer. In addition, we can vary the bending angle of the magnetic compressor, resulting in a changing R_{56} term for the chicane. Hence, a total of 7 knobs is available to control the compression and energy profile of the beam at the spreader exit.

The Pareto front in this case is a 2 dimensional curve embedded in the 3 dimensional space of bunch length, total momentum spread and slice momentum spread, the quantities to be minimized. The projection of the population of solutions in the $z_{rms} - \delta$ plane is shown in Fig. 4.

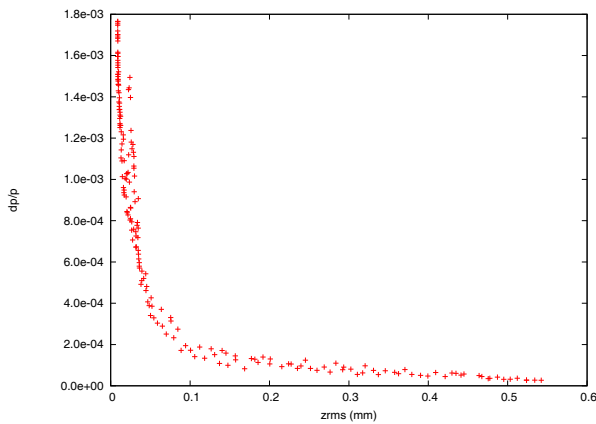


Figure 4: Pareto optimum front at the exit of the spreader (>1.8 GeV).

One significant point to be made is that although, in principle, the 3.9 GHz cavity is allowed to accelerate the beam or remove the correlated linear chirp, the optimizer favours solutions where this cavity acts as a linearizer. Hence, the algorithm is in accordance with physical intuition. This is

shown in Fig. 5.

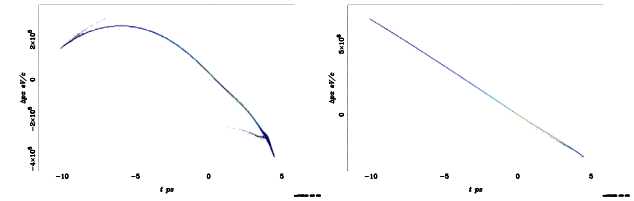


Figure 5: Typical behavior of solutions before and after the 3rd harmonic cavity. The optimizer uses it as a linearizer, as expected.

As described previously, the result of the genetic optimizer is not a single solution, but a set of solutions, all of which are optimal in the Pareto sense.

As in the case of the injector, the numerical values of the objective functions are only part of the decision process. The full phase space plots are used instead, and thus more information about the beam properties is taken into account. Two of those solutions are shown in Figs. 6 and 7.

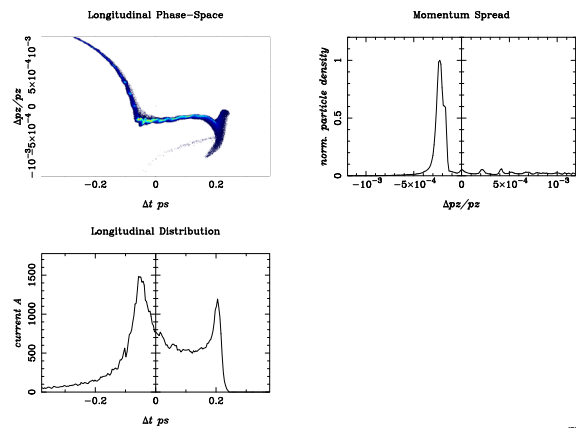


Figure 6: High compression case at the spreader exit, beam energy 1897 MeV.

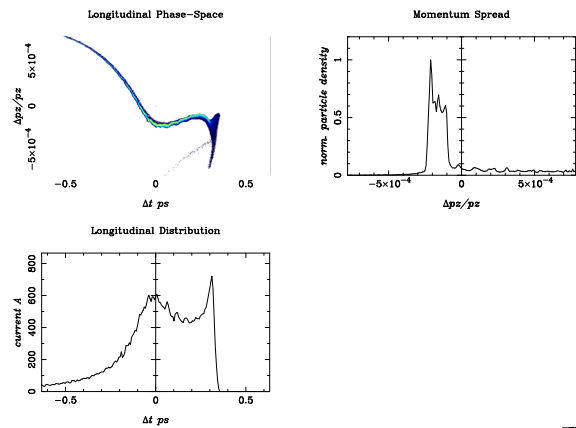


Figure 7: Low compression case at the spreader exit, beam energy 1913 MeV.

The relative merits of the two solutions plotted in Figs. 6 and 7 will be ultimately decided by simulations of the FEL process, but one common characteristic is the presence of a “good” region in the middle of the beam, with lower quality regions in the head and tail of the beam. Indeed, the next step in the optimization process will be to minimize the longitudinal tails, while increasing the quality of the good region in the middle of the beam.

DISCUSSION

The bunch charge used for the injector and linac simulations is 300 pC, and is not currently a knob in the simulations. Indeed, since the charge extracted at the cathode affects the beam quality in a fundamental way, adding it to the list of knobs adds significant complexity to the underlying physics model. Preliminary steps towards the optimization of this knob in the injector region have been taken nonetheless and are reported in [10].

One other area of interest is the presence of nonlinear longitudinal correlations coming out of the injector. These are partly responsible for the low quality regions in the head and tail of the beam, and are associated with high compression at low energies. Indeed, comparing Figs. 3 with 6 and 7, we see that the bifurcated structure at the head of the beam (to the right) is transported from the injector through the linac. In order to optimized for tails and/or higher order correlations, more complex objective functions that take into account higher order moments of the beam might be needed.

In the present study we focused exclusively on the evolution of the longitudinal phase space of the beam. The physics model includes the interaction of the beam with the rf structure fields, the rf wakefields and coherent synchrotron radiation in the bunch compressor bends (but not in the spreader bends). We did not include the effect of longitudinal space charge.

The optimizer can accommodate additional elements important for beam manipulation, such as a laser heater, used in LCLS [11] and other FEL projects to control the onset of the microbunching instability. Although included in the transport lattice used in the model, it is not a knob in the genetic optimizer. Other candidates include a tail management, or collimation system, not currently addressed in the model.

Finally, although care has been taken to ensure the numerical stability of the simulations, by its nature the optimization process requires fast calculation routines, that may not capture all the relevant phenomena. Of particular interest is the microbunching instability, and comparisons with massively parallel codes such as IMPACT [12] will be needed to verify the validity of the lower resolution optimized solutions.

In the current numerical setup, only the optimization algorithm is parallel, and individual simulations run as single threads on a single processor. In future versions of the code, the parallel capabilities of both Astra and Elegant, as

well as IMPACT, may be used as well.

CONCLUSIONS

We have presented preliminary results showing the application of an optimization tool we are developing for the design of a 4th generation x-ray light source. In particular, we focus on the injector and linac part of the the accelerator, and discuss the electron beam dynamics relevant to the transport, acceleration and longitudinal compression of the beam.

For this a parallel multiobjective optimizer is applied to the design process. The main advantage of the approach is the systematic comparison of multiple solutions, that are optimal in a Pareto sense. Possible future directions in the model development are also discussed.

REFERENCES

- [1] J. Corlett et al., TUPB26, Proc. of FEL'11, Shanghai, China.
- [2] M. Reiser, Theory and Design of Charged Particle Beams, Wiley-VCH, 2006
- [3] Ivan V. Bazarov and Charles K. Sinclair. Multivariate optimization of a high brightness dc gun photoinjector. PRSTAB, 8(3):034202+, Mar 2005.
- [4] K. Deb. Multi-objective optimization using evolutionary algorithms. Wiley, 2001.
- [5] F. Sannibale et al., THPB14, Proc. of FEL'11, Shanghai, China.
- [6] Flottmann, K., ASTRA: A space charge tracking algorithm, user's manual available at http://www.desy.de/~mpyflo/Astra_dokumentation
- [7] E. Kurr et al. “Accelerator Design Study for a Soft-X-Ray Free Electron Laser at LBNL”, LBNL Report LBNL-2670E (2009)
- [8] J. Qiang et al., Phys. Rev. ST Accel. Beams 12, 100702 (2009)
- [9] M. Borland, ELEGANT: A flexible SDDS-compliant code for accelerator simulation, Argonne National Lab Technical Report
- [10] C. F. Papadopoulos et al., TUPB13, Proc. of FEL'11, Shanghai, China.
- [11] P.Emma et al., Nature Photonics 4, 641–647 (2010)
- [12] J. Qiang et al., J. Comp. Phys. 163, 434 (2000).